

Zn²⁺ Substitution by Pb²⁺ in Alkaline-boro-aluminosilicate Glass-ceramics: Microstructural Aspects

Mrinmoy Garai^{1,2*}, Basudeb Karmakar²

¹Materials Science Centre, Indian Institute of Technology, Kharagpur, 721302, India

²Glass Science & Technology Section, Central Glass and Ceramic Research Institute, 196, Raja S. C. Mullick Road, Kolkata, 700032, India

*Corresponding author

DOI: 10.5185/amp.2018/042

www.vbripress.com/amp

Abstract

This study exemplifies the effects of 5 wt.% Pb²⁺ addition replacing the same Zn²⁺ content on crystallization and microstructure of 10B₂O₃-16Al₂O₃-39SiO₂-12MgO-12MgF₂-4K₂O-1Li₂O-1AlPO₄ (wt.%) glass-ceramic composite. Increase of linear thermal-expansion (6.93 to 7.18×10⁻⁶/K at 50-600°C) in substituting Zn²⁺ by Pb²⁺ is attributed to the field-strength of cations. Opaque crystalline glass-ceramics are derived from the transparent glasses (synthesized by single-step melt-quenching at 1500°C) by controlled heat-treatment at 1050°C and the predominant crystalline-phase was identified as fluorophlogopite mica, KMg₃AlSi₃O₁₀F₂. FFESEM of the ZnO containing glass-ceramics revealed that 100-200 μm sized plate-like crystals are in 'well-packed interlocked arrangement'; which changed to 'nanocrystalline microstructure' combined of 'spherical droplet like' nanocrystals (crystal size = 10-50 nm) in attendance of PbO. Decrease in linear thermal-expansion (11.03 to 7.93 × 10⁻⁶/K at 50-700°C) due to the substitution of ZnO is ascribed to the crystallization inhibiting tendency of PbO towards boroaluminosilicate system. Thermal-expansion of ZnO containing glass-ceramic is large (> 11 × 10⁻⁶/K at 50-700 and 50-800°C) which can exhibit their enough thermal shock resistivity to be suitable for high-temperature sealing application. Copyright © 2017 VBRI Press.

Keywords: Glass, crystallization, glass-ceramics, microstructure, thermal expansion.

Introduction

Boroaluminosilicate (BAS) glass-ceramics are technologically important material due to their large thermal expansion, thermal shock resistivity, high mechanical strength and enough chemical durability [1-3]. B₂O₃-Al₂O₃-SiO₂-MgO-MgF₂-K₂O-Li₂O-AlPO₄ is a type of glass-system, which is converted to mica glass-ceramics by controlled heat-treatment technique, in particular of the fluorophlogopite system, which impart excellent machineability, due to the layered atomic structure that causes a basal cleavage along the (001) planes of the plate-shaped crystals [4-8]. Beside the easy flexibility of formation by heat treatment in the glass matrix, these glass-ceramics have consequent reproducibility of properties from the homogeneity of as-cast melt glass. They typically contain a finite quantity of crystalline ceramic phase produced by the controlled crystallization of highly viscous glass forming melts. In the study of aluminosilicate glass-ceramic, Holand and his co-author [9] reported the precipitation of bent mica crystals apart from the house-of-cards like microstructure, in a glass with composition: 48.9 wt.% SiO₂, 27.3 wt.% Al₂O₃, 11.7 wt.% MgO, 3.2 wt.% Na₂O, 5.2 wt.% K₂O, 3.7 wt.% F. Such

type of base glass system generally produces straight plate-like crystals that finally form the house-of-cards like microstructure at the end [10]; but shows a reduced glass-in-glass phase separation tendency. As a consequence, a smaller number of nucleation sites become available for the formation of crystals than is the case in flat mica development. The encouraging processing properties associated with this glass-ceramic are attributed to different phenomena like: (i) Firstly, the fact that mica phase possesses a marked preferential cleavage plane. (ii) Secondly, the micas in the house-of-cards microstructure are positioned in close contact with one another and hence, cracks can be propagated readily within the crystals during the machining (without causing the bulk ceramic body to fracture). These mica glass-ceramics also exhibit good lubricity [9].

From the microstructural engineering point of view, the mica glass-ceramics furnish the microstructure containing excellent strength, uniformity, and enough thermal stress resistance capability. The most important features of mica based glass-ceramic are high thermal shock resistance capability and large thermal expansion coefficient (CTE), which lead to a commercial interest, in particular, for high temperature application. And, thus the

increase of CTE and shock resisting capability is of great interest for B_2O_3 - Al_2O_3 - SiO_2 - MgO - MgF_2 - K_2O - Li_2O - $AlPO_4$ glass-ceramics.

Thermal expansion of such glasses can be manipulated over a desired range by tailoring the composition, extent of crystallization; crystal morphology and crystal size [1-3]. The transition metal ions like Mn^{2+} , Ni^{2+} , Zn^{2+} etc. and p-block metal ions like Sn^{2+} , Pb^{2+} etc. possesses enough solubility in Si-O-Si glass phase and thus can be the stimulating chemical addition to B_2O_3 - Al_2O_3 - SiO_2 - MgO - MgF_2 - K_2O - Li_2O - $AlPO_4$ glass batch composition in respect of achieving the desired properties. Despite hampering the glass network considerably, the p-block metal ions can play significant role in controlling the thermal properties like glass transition temperature (T_g), softening point (T_s), thermal expansion (CTE) and density of glass due to their adequate positive (+ve) charge density as well as greater polarisability in silicate glass matrix (Si-O-Si). After crystallization in glass matrix, some amount of amorphous glassy phase always exists and the properties of glass-ceramic composite certainly depends on both the crystalline phase as well as existing amorphous phase. In the study of CaO, BaO and ZnO containing binary, ternary and quaternary silicate glasses, Kerstan *et al.* [3] established that the coefficient of thermal expansion (CTE) of glass-ceramic composite in not only affected by the CTE of the crystalline phases, but also by that of the residual glass phase significantly. For Li_2O -CaO- SiO_2 system, Tarlakov and his co-workers [4] explored the effects of CaO addition on the glass structure and crystallization mechanism and they argued that the increase of CaO content in glass matrix results in increasing the temperature interval of crystallization. In ZnO - Al_2O_3 - SiO_2 based glass-ceramics, the addition of Ba^{2+} caused a structural change which renders the Si-O-Si network of the residual glassy phase in ceramic matrix more open than Ca^{2+} and Sr^{2+} [5-8]. These are the self-proclaimed effect of bi-valent metal ions in silicate based glasses.

We are aimed to demonstrate the substitution of ZnO by PbO in $39SiO_2$ - $12MgO$ - $16Al_2O_3$ - $10B_2O_3$ - $12MgF_2$ - $4K_2O$ - $5ZnO$ - $1Li_2O$ - $1AlPO_4$ (wt.%) glass system and the relevant effects on crystallization, microstructure and thermal properties. The concerned effects of ZnO substitution on physical and thermal properties are established by means of dilatometry, X-ray diffraction and electron microscopy. On the basis of crystallization, microstructure and thermal expansion, the comparison is made for Zn^{2+} and Pb^{2+} containing B_2O_3 - Al_2O_3 - SiO_2 - MgO - MgF_2 - K_2O - Li_2O - $AlPO_4$ glasses; and the applicability of such glasses as high temperature sealing material will be indicated.

Table 1. Composition of studied ZnO and PbO containing B_2O_3 - Al_2O_3 - SiO_2 - MgO - MgF_2 - K_2O - Li_2O - $AlPO_4$ Glasses.

Sample No.	Composition (wt. %)									
	SiO_2	Al_2O_3	MgO	B_2O_3	MgF_2	Li_2O	$AlPO_4$	K_2O	ZnO	PbO
Zn-5	39	16	12	10	12	1	1	4	5	0
Pb-5	39	16	12	10	12	1	1	4	0	5

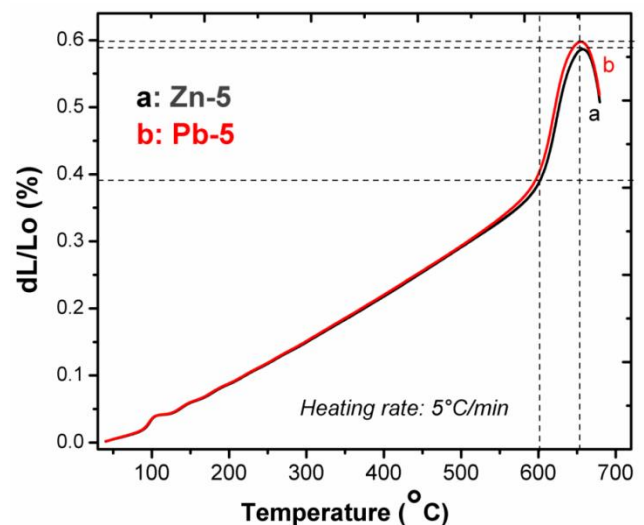


Fig. 1. Dilatometric thermograph for comparing of thermal expansion trend as a function of temperature between ZnO (Zn-5) and PbO containing (Pb-5) B_2O_3 - Al_2O_3 - SiO_2 - MgO - MgF_2 - K_2O - Li_2O - $AlPO_4$ glasses (for composition see Table 1).

Experimental

The B_2O_3 - Al_2O_3 - SiO_2 - MgO - MgF_2 - K_2O - Li_2O - $AlPO_4$ glasses were synthesized by conventional melt-quench technique at 1500°C (for 2 hr), followed by controlled heat treatment to convert into glass-ceramic. The glass batches of B_2O_3 - Al_2O_3 - SiO_2 - MgO - MgF_2 - K_2O - Li_2O - $AlPO_4$ system with ZnO or PbO content, was mixed with special attention for homogeneous dispersion of each component throughout the batch mixture. Composition of these glasses is summarized in **Table 1**. The batch mixture shown in Table 1 does not contains any room temperature volatile compounds. Because most of the required components were taken either in oxide, carbonate or hydroxide form. So, the chances of alloy formation, agglomeration or colloid formation were very less during mixing as well as melting process at 1500°C . High purity reagent grade fine chemicals were used as raw materials: SiO_2 (Quartz Powder), $Mg(OH)_2$ (97%, Loba Chemie, Mumbai, India), $Al(OH)_3$ (97%, Loba Chemie, Mumbai, India), K_2CO_3 (98%, Loba Chemie, Mumbai, India), H_3BO_3 (99.5%, Loba Chemie, Mumbai, India), MgF_2 (99.9%, Loba Chemie, Mumbai, India), $LiCO_3$ (99.9%, Loba Chemie, Mumbai, India), $AlPO_4$ (99%, Merck, Mumbai, India), $PbCO_3$ (99%, Merck, Mumbai, India) and ZnO (99%, E. Merck Ltd., Mumbai, India). The chemicals used were directly applied for glass batch preparation without any further purification. During the conventional melting process of these glasses, two stirring was performed for homogeneous mixing of the melt. To remove the internal stress, the glass melts were annealed at 620°C for 2 h and then cooled down slowly to room temperature. In order to avoid the unwilling crystallization during the transformation from melting to annealing furnace, the glass melts were sudden cooled in a preheated graphite mould in open air followed by entering into the annealing furnace. As synthesized glass monoliths after annealing was transparent in nature in visible region. The viscosity of the

Zn-5 glass was fairly higher than that of Pb-5 glass as visualized during stirring of melt at 1500°C. Annealed glasses were then heat-treated at 1050°C (for 4 hour duration) for nucleation and crystallization.

For evaluating the glass transition temperature (T_g), co-efficient of thermal expansion (CTE) and dilatometric softening point (T_d), the glass samples (cylinder shaped; length~25 mm and diameter~6 mm) were assessed under a horizontal dilatometer, NETZSCH DIL 402 PC (NETZSCH-Gerätebau GmbH, Germany) at a heating rate of 5°C/min with an accuracy of $\pm 1\%$ after calibration with a standard Al_2O_3 cylinder. The density of the different glass and glass-ceramic bulk samples were determined by Archimedes principle using distilled water as immersion liquid in a digital balance (Mettler Toledo; accuracy of $\pm 0.7\%$). X-ray diffraction (XRD) of the B_2O_3 - Al_2O_3 - SiO_2 - MgO - MgF_2 - K_2O - Li_2O - $AlPO_4$ glass and corresponding glass-ceramic samples were performed using an XPERTPRO MPD diffractometer (PANalytical, Almelo, Netherlands) operating with Ni-filtered $CuK\alpha$ ($\lambda = 1.5406 \text{ \AA}$) radiation as the X-ray source, scan range 5-90° with a step size of 0.05°, irradiated at 40 kV and 40 mA. The microstructural morphology of glass-ceramics was examined by field emission scanning electron microscopy (FESEM model S430i, LEO, CEA, USA) using finely surface polished glass-ceramic samples (chemically etched by immersion in 2 vol% aqueous HF solution for 10 min).

Results and discussion

The trend in variation of glass transition temperature (T_g), dilatometric softening temperature (T_d) and coefficient of thermal expansion (CTE) of present boroaluminosilicate glasses evaluated by dilatometric study, and the comparison of these two glasses (Zn-5 and Pb-5) in their thermal expansion pattern is exhibited in **Fig. 2**, from which estimated values are summarized in **Table 2**. In fact, the T_g and T_d values estimated are in proximate for Zn-5 and Pb-5 glasses. In case of CTE also, the value is slightly increased from 6.36 to $6.40 \times 10^{-6}/K$ at 50-500°C on addition of PbO in place of ZnO; and this small increase is ascribed to the cationic field strength [$z_c/(r_c + r_a)^2$, z_c , r_c and r_a are the charge of cation, radius of cation and radius of anion, respectively] of Zn^{2+} and Pb^{2+} ions. Similarly, at 50-600°C range, CTE of Pb-5 glass is higher by $0.25 \times 10^{-6}/K$. The increase in CTE is also associated with the increase of ionic radius of Pb^{2+} caused by the decrease of effective nuclear charge. In the study of Li_2O - ZnO - SiO_2 - Na_2O - B_2O_3 - P_2O_5 glasses, Sharma et al. [11] explained the significant variation in thermal and physical properties with the effect of $ZnO/(ZnO+SiO_2)$ ratio. In Zn-5 and Pb-5 system, total glass modifier oxide content is 17 wt.% (12 MgO + 4 K_2O + 1 Li_2O), where the alumina (Al_2O_3) content is 16 wt% and $B_2O_3 = 10$ wt%. When, entire concentration of Al_2O_3 and B_2O_3 is almost balanced by glass modifier oxide, all oxygen atoms are in bridging approach i.e., Al-O-Al, B-O-B along with Si-O-Si. Further addition of modifier oxide ZnO and PbO results in increase of non-bridging oxygen (NBOs), which directly affects the

stabilization of glass matrix to increase the glass transition region. This fact supports the glass transition temperature of Zn-5 and Pb-5 glasses as 608 and 605°C, and softening point as 657 and 656°C, respectively.

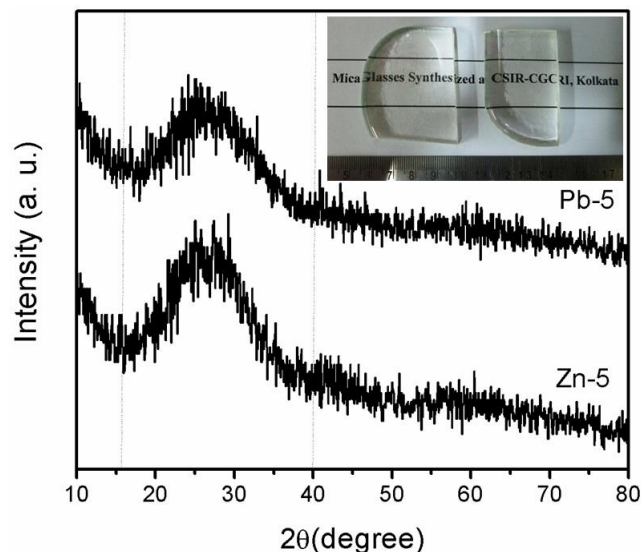


Fig. 2. X-ray diffraction (XRD) pattern of the precursor B_2O_3 - Al_2O_3 - SiO_2 - MgO - MgF_2 - K_2O - Li_2O - $AlPO_4$ glasses containing ZnO (Zn-5) and PbO (Pb-5) showing their amorphous nature in $2\theta = 15-40^\circ$; inset shows the transparent nature of the as prepared Zn-5 (left) and Pb-5 (right) glasses (for composition see Table 1).

Table 2. Dilatometric Thermal Properties, Glass Transition Temperature (T_g), Softening Point (T_d) and Coefficient of Thermal Expansion (CTE) of ZnO and PbO containing B_2O_3 - Al_2O_3 - SiO_2 - MgO - MgF_2 - K_2O - Li_2O - $AlPO_4$ glasses.

Sample No.	T_g (°C)	T_d (°C)	CTE ($\times 10^{-6}/K$)			
			50-300°C	50-400°C	50-500°C	50-600°C
Zn-5	608	657	5.78	6.08	6.36	6.93
Pb-5	605	656	5.84	6.14	6.40	7.18

Amorphous nature of the melt-quenched ZnO and PbO containing B_2O_3 - Al_2O_3 - SiO_2 - MgO - MgF_2 - K_2O - Li_2O - $AlPO_4$ glasses were studied by powder X-ray diffraction technique (XRD) in the 2θ range of 10-80° as represented in **Fig. 2**. The broad hump appeared at around (2θ) 15-40° confirms their amorphous nature. Inset of **Fig. 2** shows the transparent nature of synthesized glasses in visible region. These transparent glasses were converted into opaque glass-ceramics by controlled heat-treatment at 1050°C for 4 h duration and the developed crystalline phases in Zn-5 and Pb-5 glasses were analyzed by XRD technique as represented in **Figs. 3** and **4**, respectively. In **Fig. 3**, the characteristic peaks appeared at (2θ) 19.30, 23.09, 24.35, 26.88, 28.35, 30.24, 34.24, 40.97, 45.39, 50.23, 52.75, 54.01, 55.70, 60.33 and 63.06° correspond to the phase reflection of (020), (111), (112), (003), (112), (113), (200), (222), (005), (224), (241), (151), (313), (331) and (205) crystalline plane of potassium magnesium aluminium fluoride silicate, fluorophlogopite $KMg_3(AlSi_3O_{10})F_2$; end centered cubic lattice, monoclinic system, cell parameter $a = 5.299$, $b = 9.188$, $c = 10.13$, molecular

weight = 421.24 (JCPDS file number 71-1542). At high temperature (1050°C), Zn^{2+} has enough solubility to SiO_4^{4-} anions, so it tends to form a solid solution with Si-O-Si glass phase and MgO to develop a Mg, Si and Zn-enriched crystalline phase. As seen from **Fig. 3**, the characteristic peaks appeared at (2 θ) 24.35, 26.88, 28.35, 30.24, 34.24, 36.76 and 63.06° correspond to the phase reflection of (311), (121), (221), (321), (002), (302) and (523) planes of zinc magnesium silicate, $\text{ZnMgSi}_2\text{O}_6$, orthorhombic primitive system, molecular weight = 241.85; lattice parameter $a = 18.20$, $b = 8.916$, $c = 5.209$ (JCPDS file number 70-0853).

Three highest intense crystalline peaks at (2 θ) 28.35, 30.24 and 34.24° appeared in the XRD of Zn-5 glass-ceramic (**Fig. 3**) are signifying the predominant formation of fluorophlogopite mica; but the intensity of these peaks is rather large due to the additional phase reflection for Mg and Si-enriched crystalline phases [12, 13], magnesium silicate 'Enstatite', MgSiO_3 , molecular weight = 100.39, orthorhombic primitive system; JCPDS file number 11-0273 (lattice parameter $a = 9.25$, $b = 8.74$, $c = 5.32$). During the crystallization in B_2O_3 - Al_2O_3 - SiO_2 - MgO - MgF_2 - K_2O - Li_2O - AlPO_4 glass, Mg^{2+} ion preferentially accommodates in octahedral coordination (ionic radius of $\text{Mg}^{2+} = 0.72$ Å) in crystal structure of fluorophlogopite mica. Zn^{2+} having similar ionic radii with Mg^{2+} in four coordination ($\text{Mg}^{2+} \sim 0.58$ Å, $\text{Zn}^{2+} \sim 0.60$ Å) as well as six coordination number ($\text{Mg}^{2+} \sim 0.72$ Å, $\text{Zn}^{2+} \sim 0.75$ Å), gets an opportunity to form Zn-mica, $\text{KZn}_3(\text{AlSi}_3\text{O}_{10})\text{F}_2$. But, at such higher temperature, it tends to exhibit its strong preference to form a solid solution with $[\text{SiO}_4]^{4-}$ ion, leading to the development of zinc silicate (Willemite, Zn_2SiO_4). Thus, some higher intense peaks appeared at (2 θ) 31.25, 54.01, 55.70, 60.33 and 71.27° in **Fig. 3** is ascribed to the development of Zn and Si-enriched crystalline phase, zinc silicate 'Willemite' (Zn_2SiO_4); JCPDS file number 70-1235, hexagonal system, rhomb centered lattice, molecular weight = 222.84, lattice parameter $a = 13.94$, $c = 9.315$ [12].

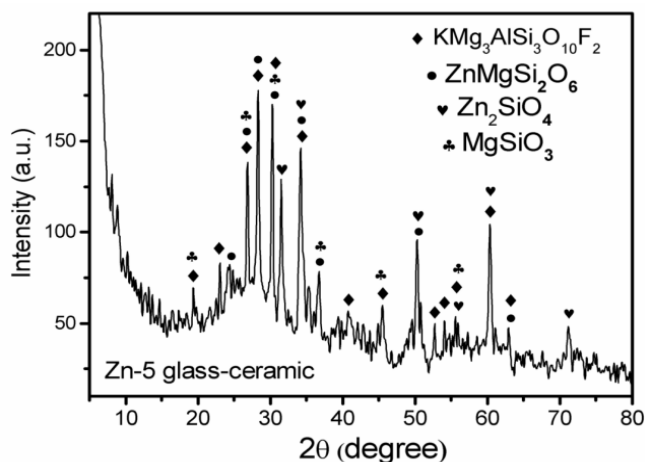


Fig. 3. X-ray diffraction (XRD) pattern of ZnO containing B_2O_3 - Al_2O_3 - SiO_2 - MgO - MgF_2 - K_2O - Li_2O - AlPO_4 glass-ceramic (Zn-5) heat treated at 1050°C; showing the appearance of crystalline phases $\text{KMg}_3(\text{AlSi}_3\text{O}_{10})\text{F}_2$ (JCPDS 71-1542), $\text{ZnMgSi}_2\text{O}_6$ (JCPDS 70-0853), Zn_2SiO_4 (JCPDS 70-1235) and MgSiO_3 (JCPDS 11-0273).

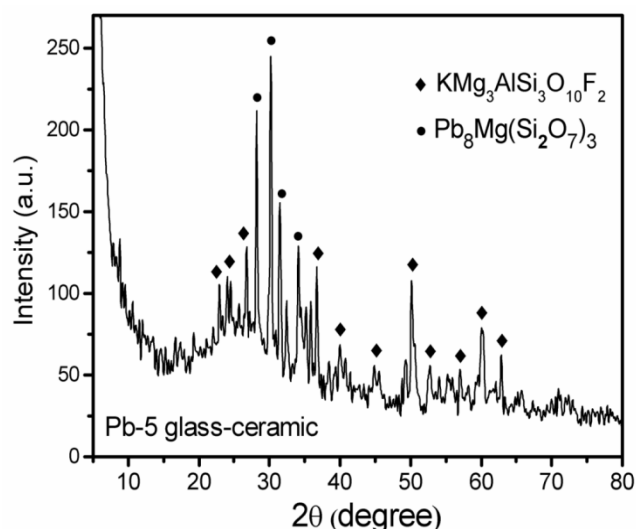


Fig. 4. X-ray diffraction (XRD) pattern of PbO containing B_2O_3 - Al_2O_3 - SiO_2 - MgO - MgF_2 - K_2O - Li_2O - AlPO_4 glass-ceramic (Pb-5) heat treated at 1050°C; showing the appearance of crystalline phases $\text{KMg}_3(\text{AlSi}_3\text{O}_{10})\text{F}_2$ (JCPDS 71-1542) and $\text{Pb}_8\text{Mg}(\text{Si}_2\text{O}_7)_3$ (JCPDS 32-0525).

In case of XRD of PbO containing glass-ceramic represented in **Fig. 4**, the characteristic peaks appeared at (2 θ) 22.98, 24.29, 26.69, 28.22, 30.18, 34.10, 39.99, 45.44, 50.23, 52.85, 54.16, 55.47, 56.99 and 60.26° are corresponding to fluorophlogopite mica, $\text{KMg}_3(\text{AlSi}_3\text{O}_{10})\text{F}_2$ (JCPDS file no. 71-1542). To unveil the miscibility of Pb^{2+} and Mg^{2+} in homogeneous Si-O-Si matrix, the Pb, Si and Mg-enriched phase is developed in Pb-5 glass matrix. As seen from **Fig. 4**, the characteristic peaks appeared at (2 θ) 22.98, 28.22, 30.18, 31.48, 32.36, 49.14 and 54.16° are corresponding to the phase reflection from (116), (122), (125), (300), (217), (410) and (2119) planes of lead magnesium silicate, $\text{Pb}_8\text{Mg}(\text{Si}_2\text{O}_7)_3$, molecular weight = 2186.41, hexagonal rhomb-centered system, lattice parameter $a = 9.739$, $c = 38.27$ (JCPDS file number 32-0525). One clear point is remarked from **Figs. 3** and **4**, that both the glasses are sufficiently crystallized on heat-treatment at 1050°C to convert into polycrystalline glass-ceramic, where fluorophlogopite mica predominates as primary crystalline phase.

Thermal properties of silicate based glasses are significantly altered when converted into polycrystalline glass-ceramics because of their composition is changed when crystallized. In order to resolve the change in microstructural morphology in ZnO and PbO containing B_2O_3 - Al_2O_3 - SiO_2 - MgO - MgF_2 - K_2O - Li_2O - AlPO_4 glass ceramics heat-treated at 1050°C, the field emission scanning electron microscopy (FESEM) was performed as presented in **Figs. 5 (a, a')** and **(b, b')**, respectively. In view of XRD study, the glasses are sufficiently converted to polycrystalline glass-ceramics containing fluorophlogopite mica, $\text{KMg}_3(\text{AlSi}_3\text{O}_{10})\text{F}_2$ phases predominately. As noticed from **Fig. 5 (a, a')**, Zn-5 glass-ceramic is composed of 50-200 μm plate like fluorophlogopite mica ($\text{KMg}_3\text{AlSi}_3\text{O}_{10}\text{F}_2$) crystals dispersed throughout the matrix. Large number of plate like mica crystals are constrained to be interlocked

(Fig. 5a') that they formed a highly compact microstructure. Such adequate crystalline growth in Zn-5 glass-ceramic explains the ascending of bigger sized crystals due to the addition of zinc (Zn^{2+}) ions. Quite variation in crystalline morphology is comprehended in detail look of Fig. 5a' which directly supports the XRD result i.e. the development of different crystalline phases viz. zinc magnesium silicate, $\text{ZnMgSi}_2\text{O}_6$, enstatite (MgSiO_3), and willemite (Zn_2SiO_4) in addition to fluorophlogopite mica $\text{KMg}_3(\text{AlSi}_3\text{O}_{10})\text{F}_2$. For similar type of $\text{K}_2\text{O}-\text{B}_2\text{O}_3-\text{Al}_2\text{O}_3-\text{SiO}_2-\text{MgO}-\text{F}$ based glass system, Molla et al. [16] obtained polycrystalline glass-ceramic containing 70% crystalline morphology after heat-treatment at 1040°C for 12 h duration.

Concerning the higher concentration of B_2O_3 in present boroaluminosilicate glasses (10 wt.%), the B^{3+} ion (ionic radius = 0.20 \AA and atomic weight = 10.81) can be expected to enter into the tetrahedral layer of fluorophlogopite phase substituting Si^{4+} (ionic radius = 0.41 \AA and atomic radius = 28.09) to develop B-mica i.e. $\text{K}[\text{Mg}_3(\text{Al,B})\text{Si}_3\text{O}_{10}]\text{F}_2$ [14]. However, in present case no boron containing mica phase is identified from XRD result. All B_2O_3 content is present in glass phase, B-O-B. In case of Zn-5 system, Zn^{2+} forms zinc silicate beating Zn-mica due to having strong preference towards silicate, SiO_4^{4-} anion. When, PbO is added in $\text{B}_2\text{O}_3-\text{Al}_2\text{O}_3-\text{SiO}_2-\text{MgO}-\text{MgF}_2-\text{K}_2\text{O}-\text{Li}_2\text{O}-\text{AlPO}_4$ glass substituting ZnO; an exceeding change in the crystalline morphology is observed as is evident in Fig. 5 (b, b'). The longer sized plate shaped mica crystals are dissolved into the Si-O-Si/B-O-B glass phase to form nanocrystalline agglomerates. Fig. 5b clearly demonstrates the liquid-liquid phase separation which occurs near 800°C ; and the liquid droplets appeared very small and randomly dispersed over the glass matrix. Yekta et al. [15] argued that the addition of PbO to the aluminosilicate glass changed the mica crystalline morphology from platelet to spherical shape. This fact can obviously be attributed to the atomic volume and charge of lead ion (Pb^{2+}). As is evident from Fig. 5b', the 30-50 nm sized droplet like crystals are suspended in boroaluminosilicate glass matrix. Here, glass phase seems to be predominant over crystalline phases to appear the unique type morphology like 'floating of mica nanocrystals in the sea of amorphous glass matrix'. Lead magnesium silicate, $\text{Pb}_8\text{Mg}(\text{Si}_2\text{O}_7)_3$ phase is also developed in this glass-ceramic in addition to fluorophlogopite, $\text{KMg}_3(\text{AlSi}_3\text{O}_{10})\text{F}_2$ mica; still the crystallinity seems to be less than 40%.

Now, the interlocked type microstructure (Fig. 5a') developed in Zn-5 glass-ceramic evokes the obsessive concern for ZnO addition in $\text{B}_2\text{O}_3-\text{Al}_2\text{O}_3-\text{SiO}_2-\text{MgO}-\text{MgF}_2-\text{K}_2\text{O}-\text{Li}_2\text{O}-\text{AlPO}_4$ system for high temperature application. Such interlocked type microstructure attains sufficient thermal shock resistivity as a sealing material in order to prevent the generation and growth of a micro-crack during thermal recycling operation in high temperature application like solid oxide fuel cell (SOFC).

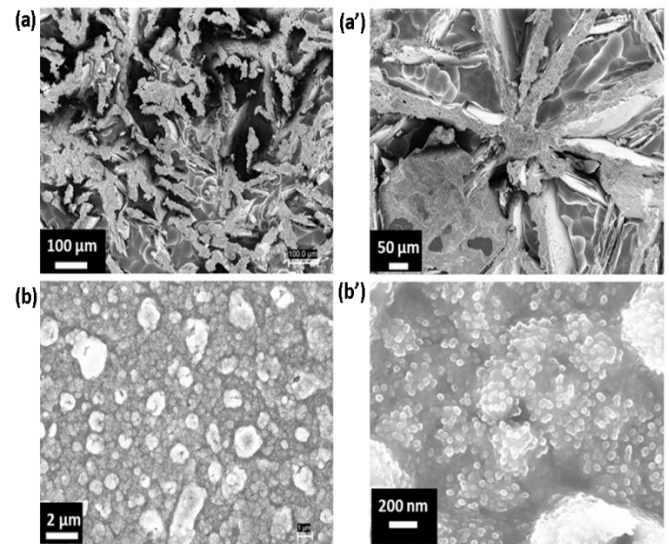


Fig. 5. FESEM microstructure of etched (by immersion in 2 vol% aqueous HF solution for 5 min) $\text{B}_2\text{O}_3-\text{Al}_2\text{O}_3-\text{SiO}_2-\text{MgO}-\text{MgF}_2-\text{K}_2\text{O}-\text{Li}_2\text{O}-\text{AlPO}_4$ glass-ceramic containing 5 wt.% ZnO (a, a') and 5 wt.% PbO (b, b') (for composition see Table 1).

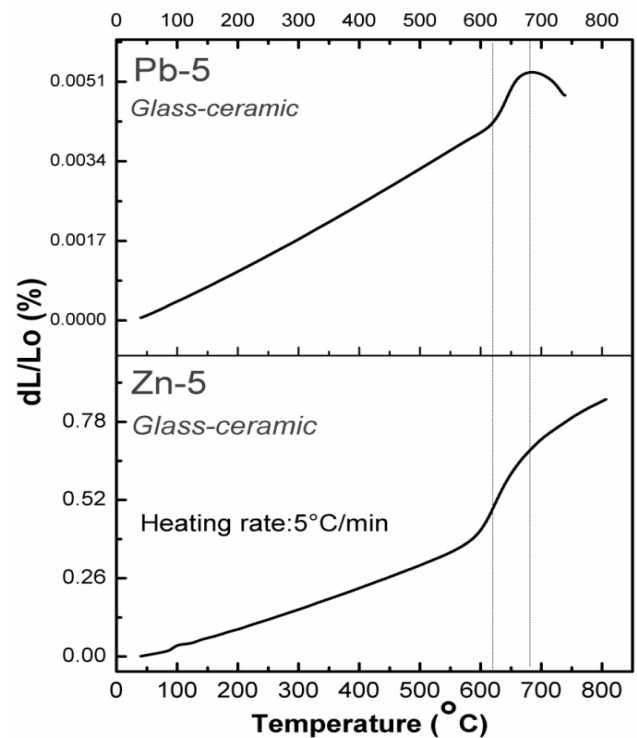


Fig. 6. Linear variation of thermal expansion with temperature for ZnO and PbO containing $\text{SiO}_2-\text{MgO}-\text{Al}_2\text{O}_3-\text{B}_2\text{O}_3-\text{MgF}_2-\text{K}_2\text{O}-\text{Li}_2\text{O}-\text{AlPO}_4$ glasses after heat-treatment at 1050°C ; Zn-5 showing crystallized nature but Pb-5 showing glassy nature possessing certain glass transition region (for composition see Table 1).

For aluminosilicate based glass-ceramics, coefficient of thermal expansion (CTE) value is significantly dependent on the nature and amount of crystalline phases present. In Fig. 6, the linear increasing trend in thermal expansion is seen for both the studied glass-ceramics heat-treated at 1050°C ; however, the value is decreased when ZnO is substituted by PbO. Zn-5 glass-ceramic possess

CTE value $5.71 \times 10^{-6}/\text{K}$ at 50-300°C and it increases linearly up to 800°C. Due to the presence of 5 mol% ZnO, zinc silicate (Zn_2SiO_4) crystallization is initiated in addition to fluorophlogopite mica. As is experimental from FESEM morphology, the fluorophlogopite mica and zinc silicate crystals in their crystalline arrangement are well-packed; it significantly affects in lowering the thermal expansion value. At 50-300 and 50-500°C, CTE is 6.05 and $6.63 \times 10^{-6}/\text{K}$, respectively for Zn-5 system. At temperature 50-700 and 50-800°C, CTE of this glass-ceramic is quite higher, 11.03 and $11.25 \times 10^{-6}/\text{K}$, respectively; which supports Zn-5 glass-ceramic for using as high temperature sealing material. For 5 wt.% PbO containing glass-ceramic, thermal expansion value is evaluated as 6.25, 6.51 6.96 and $7.93 \times 10^{-6}/\text{K}$, at 50-200, 50-300, 50-500 and 50-700°C, respectively. But, one vital fact in the thermal expansion trend for Pb-5 depicted in Fig. 6 that, it is looking like glassy nature. This is due to large amount of amorphous phase is existent in Pb-5 glass-ceramic microstructure as depicted as '*floating of mica nanocrystals in the sea of amorphous glass matrix*'. Hence, amount of glass phase is more than that of the crystalline part and this is the reason of such trend in thermal expansion for Pb-5 glass-ceramic. From dilatometric analysis, Liu et al. [17] observed the increase of thermal expansion coefficient by the addition of a small amount of crystalline phase phlogopite mica on sintered phlogopite mica/ $\text{SiO}_2\text{-Al}_2\text{O}_3\text{-B}_2\text{O}_3\text{-BaO-Li}_2\text{O}$ glass blends. In case of present glass-ceramics, the CTE trend is Pb-5 > Zn-5 at the temperature range 50-200, 50-300 and 50-500°C. At temperature range over glass transition region, 50-700 and 50-800°C the CTE is: Zn-5 > Pb-5 glass-ceramic. This inconsistency can be attributed to the stabilization of crystalline phase in glass-ceramic matrix [18]. The nature of Pb-5 CTE curve is minutely like a glass material, possessing a glass-transition like region. But Zn-5 glass is sufficiently converted into glass-ceramic and the CTE curve also follows a linear increasing trend with temperature [19, 20]. The fact that CTE of Pb-5 glass-ceramic increased up to 500°C and then decreased, directly point out that lead ion (Pb^{2+}) comprise a crystallization opposing tendency for boroaluminosilicate system $\text{B}_2\text{O}_3\text{-Al}_2\text{O}_3\text{-SiO}_2\text{-MgO-MgF}_2\text{-K}_2\text{O-Li}_2\text{O-AlPO}_4$. Whereas, zinc ion (Zn^{2+}) supports the crystallization in boroaluminosilicate system with the formation of larger sized crystals, i.e. facilitate the additional crystalline growth [18-23].

To act as a sealing material in high temperature application, linear increase of thermal expansion is necessary to avoid the generation and growth of micro-crack. Moreover the sealant material needs to possess higher thermal expansion coefficient matching with other materials in the operation. For Zn-5 glass-ceramic, the thermal expansion value is linearly increased up to 800°C; and the values are also very high ($> 11 \times 10^{-6}/\text{K}$ at 50-700 and 50-800°C) which is in well matching with other solid oxide fuel cell (SOFC) materials like yttria stabilized zirconia (YSZ) electrolyte, crofer 22 APU interconnect etc. Thus, 5 wt% ZnO containing $\text{B}_2\text{O}_3\text{-Al}_2\text{O}_3\text{-SiO}_2\text{-MgO-}$

$\text{MgF}_2\text{-K}_2\text{O-Li}_2\text{O-AlPO}_4$ glass (Zn-5) can be useful as a sealing material for high temperature application like SOFC [17].

Conclusion

ZnO content (5 wt.%) of $39\text{SiO}_2\text{-5ZnO-12MgO-16Al}_2\text{O}_3\text{-10B}_2\text{O}_3\text{-12MgF}_2\text{-4K}_2\text{O-1Li}_2\text{O-1AlPO}_4$ (wt.%) glass is substituted by PbO; and the relevant changes of crystallization, microstructure and thermal properties have been investigated. No significant change in the glass transition temperature, softening point as well as thermal expansion is estimated for ZnO and PbO containing glasses. Transparent $\text{B}_2\text{O}_3\text{-Al}_2\text{O}_3\text{-SiO}_2\text{-MgO-MgF}_2\text{-K}_2\text{O-Li}_2\text{O-AlPO}_4$ glasses are converted into opaque glass-ceramics on controlled heat-treatment at 1050°C and the predominant crystalline phase is identified as fluorophlogopite mica, $\text{KMg}_3\text{AlSi}_3\text{O}_{10}\text{F}_2$. Zinc magnesium silicate, $\text{ZnMgSi}_2\text{O}_6$ and willemite, Zn_2SiO_4 crystals are also developed in glass-ceramic when contains ZnO. Replacement of ZnO by PbO results in the formation of lead magnesium silicate, $\text{Pb}_8\text{Mg}(\text{Si}_2\text{O}_7)_3$. ZnO containing glass-ceramic is composed of 50-200 μm sized plate like fluorophlogopite mica ($\text{KMg}_3\text{AlSi}_3\text{O}_{10}\text{F}_2$) crystals dispersed throughout the glass-ceramic matrix. The plate like mica crystals are constrained to be interlocked to form a compact microstructure. Replacement of ZnO by PbO causes the exceeding change in the crystalline morphology where the longer sized plate shaped mica crystals are dissolved into the Si-O-Si glass phase to form nanocrystalline agglomerate. And the glass phase seems to be predominant over crystalline phases to appear the unique type morphology like '*floating of mica nanocrystal in sea of amorphous glass matrix*'. Zinc ion (Zn^{2+}) facilitates the additional crystalline growth in the formation of larger sized crystals. Thermal expansion value of ZnO containing glass-ceramic is linearly increased up to 800°C; and the values are also very high ($> 11 \times 10^{-6}/\text{K}$ at 50-700 and 50-800°C) which is suitable for high temperature sealing application like solid oxide fuel cell (SOFC). Thus, 5 wt% ZnO containing $\text{B}_2\text{O}_3\text{-Al}_2\text{O}_3\text{-SiO}_2\text{-MgO-MgF}_2\text{-K}_2\text{O-Li}_2\text{O-AlPO}_4$ glass can be a useable for high temperature sealing purpose.

Acknowledgements

The authors thank Dr. K. Muraleedharan, Director, Dr. R. Sen, Head, Glass Division of CSIR-Central Glass and Ceramic Research Institute (CGCRI), for their encouragement to carry out this work. MG thankfully acknowledges Science and Engineering Research Board (SERB) for providing financial support under National Post-Doctoral Fellowship scheme (Reference Number: PDF/2016/003799) at Materials Science Centre, Indian Institute of Technology (IIT), Kharagpur.

Author's contributions

Conceived the plan: bk; Performed the experiments: mg; Data analysis: mg, bk; Wrote the paper: mg. Authors have no competing financial interests.

References

1. Grossman, D. G. *J. Am. Ceram. Soc.* **1972**, 55, 446.
2. Hsiang, H.-I.; Yung, S. W.; Wang, C. C. *Mater. Res. Bull.* **2014**, 60, 730.
3. Kerstan, M.; Muller, M. *Mater. Res. Bull.* **2011**, 46, 2456.
4. Garai, M.; Karmakar, B. *Asian J. Mater. Chem.* **2016**, 1, 33.
5. Hamzawy, E. M. A.; Darwish, H.; *Mater. Chem. Phys.* **2001**, 71, 70.
6. Hoda, S. N.; Beall, G. H. "Alkaline Earth Mica Glass-ceramics" In: J. H. Simmons, D. R. Uhlmann, G. H. Beall (Editors), *Advances in Nucleation and Crystallization in Glasses*, The American Ceramic Society, Westerville, (1982) pp. 287-300.
7. da Silveira, C. B.; de Campos, S. D.; de Castro, S. C.; Kawano, Y. *Mater. Res. Bull.* **1999**, 34, 1661.
8. McMillan, P. W.; Partridge, G. J. *Mater. Sci.* **1972**, 7, 847.
9. Holand, W.; Rheinberger, V.; Schweiger, M. *Adv. Eng. Mater.* **2001**, 3, 10.
10. Garai, M.; Sasmal, N.; Molla, A. R.; Singh, S. P.; Tarafder, A.; Karmakar, B.; *J. Mater. Sci.* **2014**, 49, 1612.
11. Sharma, B. I.; Goswami, M.; Sengupta, P.; Shrikhande, V. K.; Kale, G. B.; Kothiyal G. P. *Mater. Lett.* **2004**, 58, 2423.
12. Mukherjee, D. P.; Das, S. K. *Ceram. Int.* **2014**, 40, 12459.
13. Sasikala, T. S.; Pavithran, C.; Sebastian, M. T. *J. Mater. Sci.: Mater. Elec.* **2010**, 21, 141.
14. Stubican, V.; Roy, R. *Am. Miner.* **1961**, 46, 32.
15. Eftekhari Yekta, B.; Hashemi Nia, S.; Alizadeh, P. *J. Eu. Ceram. Soc.* **2005**, 25, 899.
16. Molla, A. R.; Kumar, B. V. M.; Basu, B.; *J. Eu. Ceram. Soc.* **2009**, 29, 2481.
17. Liu, C. K.; Lin, K. F.; Lee, R. Y. *ECS Tran.* **2011**, 35, 2519.
18. Garai, M.; Sasmal, N.; Karmakar, B. *Ind. J. Mater. Sci.* **2015**, 638341, 1.
19. Salman, S. M.; Salama, S. N.; Abo-Mosallam, H. A. *Ceram. Int.*, <https://doi.org/10.1016/j.ceramint.2017.04.116>.
20. Garai, M.; Sasmal, N.; Molla, A. R.; Tarafder, A.; Karmakar, B. *J. Mater. Sci. Tech.* **2015**, 31, 110.
21. Liu, S.; Zhao, G.; Ying, H.; Wang, J.; Han, G.; *J. Non-Cryst. Solid.* **2008**, 354, 956.
22. Garai, M.; Sasmal, N.; Molla, A. R.; Karmakar, B., *Solid State Sci.* **2015**, 44, 10.
23. Garai, M.; Karmakar, B.; *J. Alloys Compd.* **2016**, 678, 360.